THE JOURNAL OF BIOLOGICAL CHEMISTRY VOL. 291, NO. 6, pp. 3076–3089, February 5, 2016

Progesterone-induced Acrosome Exocytosis Requires Sequential Involvement of Calcium-independent Phospholipase $A_2\beta$ ($iPLA_2\beta$) and Group X Secreted Phospholipase A_2 ($sPLA_2$)*

Received for publication, July 15, 2015, and in revised form, December 10, 2015 Published, JBC Papers in Press, December 11, 2015, DOI 10.1074/jbc.M115.677799

Roland Abi Nahed[‡§1], Guillaume Martinez[‡§1], Jessica Escoffier[‡§], Sandra Yassine[‡§], Thomas Karaouzène[‡§], Jean-Pascal Hograindleur[‡§], John Turk[¶], George Kokotos[‖], Pierre F. Ray[‡§], Serge Bottari[‡§‡‡], Gérard Lambeau[§§‖‖], Sylviane Hennebicq[‡§‖‖], and Christophe Arnoult[‡§2]**

From the [‡]Université Grenoble Alpes, F-38000 Grenoble, France, the [§]Institut Albert Bonniot, INSERM U823, La Tronche F-38700, France, the [**]Centre Hospitalier Universitaire de Grenoble, Unité Fonctionnelle de Biochimie et Génétique Moléculaire, Grenoble F-38000, France, the [¶]Division of Endocrinology, Metabolism and Lipid Research, Washington University School of Medicine, St. Louis, Missouri 63110, the [‖]Department of Chemistry, University of Athens, Panepistimiopolis, Athens 15771, Greece, the [‡‡]Centre Hospitalier Universitaire de Grenoble, Plate-forme de Radioanalyse, IBP, CS10217, Grenoble F-38000, France, the [§§]Université de Nice-Sophia Antipolis, Valbonne 06560, France, the [¶¶]Institut de Pharmacologie Moléculaire et Cellulaire CNRS UMR 7275, 06560 Valbonne, France, and the [‖‖]Centre Hospitalier Universitaire de Grenoble, Centre d'AMP-CECOS, CS1021, Grenoble F-38000, France

Phospholipase A_2 (PLA_2) activity has been shown to be involved in the sperm acrosome reaction (AR), but the molecular identity of PLA_2 isoforms has remained elusive. Here, we have tested the role of two intracellular ($iPLA_2\beta$ and cytosolic $PLA_2\alpha$) and one secreted (group X) PLA_2s in spontaneous and progesterone (P4)-induced AR by using a set of specific inhibitors and knock-out mice. $iPLA_2\beta$ is critical for spontaneous AR, whereas both $iPLA_2\beta$ and group X secreted PLA_2 are involved in P4-induced AR. Cytosolic $PLA_2\alpha$ is dispensable in both types of AR. P4-induced AR spreads over 30 min in the mouse, and kinetic analyses suggest the presence of different sperm subpopulations, using distinct PLA_2 pathways to achieve AR. At low P4 concentration (2 μM), sperm undergoing early AR (0–5 min post-P4) rely on $iPLA_2\beta$, whereas sperm undergoing late AR (20–30 min post-P4) rely on group X secreted PLA_2. Moreover, the role of PLA_2s in AR depends on P4 concentration, with the PLA_2s being key actors at low physiological P4 concentrations ($\leq$2 μM) but not at higher P4 concentrations ($\sim$10 μM).

The acrosome reaction (AR)[3] is an exocytotic and mandatory event occurring in the cumulus mass or on the zona pellucida of the oocyte and allowing the release of several types of sperm enzymes. The release of these enzymes leads to a partial hydrolysis of the layers surrounding the oocyte, allowing the sperm to reach the oolema where the fusion between the two gametes occurs. The physiological agonists of the AR and their respective downstream molecular pathways are the subject of intense investigation (1, 2). Two main physiological agonists were identified as follows: progesterone (P4), which is released by the cells of the cumulus mass, and ZP3, one of the glycoproteins of the zona pellucida (ZP) (3–5). However, for most fertilizing mouse sperm, the AR is triggered before contact with the ZP (6), and acrosome-reacted sperm are able to freely cross both the cumulus and the ZP (7), strongly suggesting that AR occurs before reaching the ZP and that P4 may be the main physiological effector of mouse AR *in vivo*. As in most exocytotic processes, Ca^{2+} plays a central role, and blocking the increase of $[Ca^{2+}]$ completely inhibits the AR. It is accepted that the main targets of Ca^{2+} are specific calcium-binding proteins such as synaptotagmin (8, 9), even if Ca^{2+} also activates calmodulin-dependent enzymes such as PI3K, whose inactivation blocks the AR (10). Numerous agonist-dependent actors involved in $[Ca^{2+}]$ increase have been characterized, including Ca^{2+} influx through activation of voltage-dependent calcium channels and store-operated channels and calcium release from the acrosome itself through activation of PLCδ4 and the inositol 1,4,5-trisphosphate receptor (2, 11–13). Contrary to neuronal exocytosis where $[Ca^{2+}]$ increase is followed within milliseconds by degranulation, sperm granule exocytosis spreads over 30 min in the presence of the agonists. Several molecular pathways are activated during the first few minutes that are mandatory for the sperm AR, including PLA_2. These enzymes catalyze the hydrolysis of phospholipids at the *sn*-2 position and generate lysophospholipids and free fatty acids that are precursors of different lipid mediators. The involvement of PLA_2 in AR was first suggested 30 years ago by experiments showing that a PLA_2 activity was associated with mouse acrosomal membranes and was inhibited by nonspecific PLA_2 inhibitors such as indomethacin, sodium meclofenamate, mepacrine, and *p*-bromophenacyl bromide (14). The role of PLA_2 was reinforced by indirect results showing that fatty acids and lysophospholipids could trigger the acrosome reaction (15–17). By using ^{14}C-la-

* This work was supported by CNRS (to C. A. and G. L.), Agence Nationale de la Recherche Grant ANR-10-EMMA-042. The authors declare that they have no conflicts of interest with the contents of this article.

[1] Both authors contributed equally to this work.

[2] To whom correspondence should be addressed: Team "Genetic, Epigenetic and Therapies of Infertility," Institut Albert Bonniot, INSERM U823, University Grenoble Alpes, 38000 Grenoble, France. Tel.: 33-476637408; E-mail: Christophe.arnoult@ujf-grenoble.fr.

[3] The abbreviations used are: AR, acrosome reaction; PLA_2, phospholipase A_2; $cPLA_2$, cytosolic phospholipase A_2; $iPLA_2$, Ca^{2+}-independent phospholipase A_2; $sPLA_2$, secreted phospholipase A_2; mGX, mouse group X secreted phospholipase A_2; P4, progesterone; ZP, zona pellucida; Pyr-1, pyrrolidine-1; SAR, spontaneous AR; BEL, *S*-bromoenol lactone.

beled fatty acids, Roldan and Fragio (18) showed that fatty acids are released during the AR of ram sperm and that RO314493, a PLA_2 inhibitor, blocked both fatty acid release and the acrosome reaction. Similar results were found in guinea pig sperm, where progesterone or ZP-induced fatty acid release and the AR were blocked by aristolochic acid, another PLA_2 inhibitor (19). Another study showed that the mouse AR is also blocked by ONO RS-82, a different PLA_2 inhibitor (20). Taken together, these studies showed that the activation of PLA_2 plays a central role in the AR and that the production of fatty acids and/or lysophospholipids is required for acrosomal and plasma membrane fusion during the AR.

At this time, however, the molecular identification of the PLA_2 isoforms involved in the AR observed in these pharmacological studies was impossible due to the lack of data regarding the specificity of the above used PLA_2 inhibitors. Indeed, the PLA_2 superfamily comprises now 37 different enzymes, divided into 16 groups and many more subgroups. It includes six distinct major types of enzymes, namely the cytosolic PLA_2s ($cPLA_2$) and the Ca^{2+}-independent PLA_2s ($iPLA_2$), both groups being intracellular, the secreted PLA_2s ($sPLA_2$), and more specific groups such as the platelet-activating factor acetylhydrolases, the lysosomal PLA_2s, and the adipose PLA_2 (21, 22). Both intracellular and secreted PLA_2s have been identified in mouse and human sperm cells (23–26). In mature mouse sperm, the group X $sPLA_2$ (mGX) is located in the acrosome and is released during the AR (24). It specifically improves fertilization and early embryo development (24, 27, 28).

PLA_2s are involved in numerous physiological processes (29, 30), and one of the challenging questions regarding PLA_2s is their respective contribution to cellular functions. The pharmaceutical industry has made significant efforts to design specific PLA_2 inhibitors with the highest possible affinity (22) to control PLA_2 activity in different pathological contexts. Among the different emerging drugs, the following drugs with reported specificities represent valuable tools to decipher the role of each PLA_2 isoform in the AR. For $sPLA_2$, LY329722 is an interesting compound, which was developed from a lead compound, LY311727, a very potent inhibitor of human group IIA $sPLA_2$ (31). LY329722 inhibits several subgroups of $sPLA_2$ (I/II/V/X) and has an IC_{50} of 30 nM for the group X $sPLA_2$ *in vitro*. For $iPLA_2$, two inhibitors emerged, *S*-bromoenol lactone (BEL) and FKGK18. BEL is a selective and irreversible inhibitor of $iPLA_2\beta$ with a half-maximal inhibition of around 60 nM after preincubation (32). Although it is a potent inhibitor of $iPLA_2\beta$, BEL also inhibits non-PLA_2 enzymes (33). For this reason FKGK18, a recently characterized $iPLA_2\beta$ inhibitor presenting fewer off-target effects with a similar potency, was identified (33). Finally, pyrrolidine-1 (Pyr-1), a pyrrolidine-based inhibitor, was identified to inhibit $cPLA_2\alpha$ (IC_{50} = 70 nM). *In vitro* assays showed that it is less potent toward $cPLA_2\gamma$ and $iPLA_2\beta$ (IC_{50} ~10 μM) and that 10 μM Pyr-1 has no inhibitory effect on group IIA, V, and X secreted PLA_2s (34).

Because of the presence of a least three different PLA_2s in sperm (23, 24, 26), and because a cross-talk between different PLA_2s has been described (35), we assessed the possible involvement of several PLA_2s during P4-induced AR in mouse sperm cells. If several PLA_2s are involved, then their respective contributions and their time of action should be characterized. Herein, we show for the first time that two PLA_2s are required during the mouse AR, $iPLA_2\beta$ and mouse group X $sPLA_2$ (mGX). Conversely, $cPLA_2\alpha$ does not appear to be involved. Interestingly, we showed that the overall contribution of PLA_2 in the AR depends on P4 concentration.

Experimental Procedures

Biological Preparation—All animal procedures were performed according to the French guidelines on the use of living animals in scientific investigations with the approval of the local Ethical Review Committee. mGX-KO mice (null for *Pla2g10* gene) on a C57BL/6J background were obtained from Lexicon Inc. as described (36). $cPLA_2\alpha$ KO mice (null for the *Pla2g4a* gene) were obtained as described (37). $iPLA_2\beta$ KO mice (null for the *Pla2g6a* gene) were obtained as described previously (23). All other mice (OF1 strain, 2–6 months old) were from Charles River Laboratories (Les Oncins, France).

Sperm Analysis, Morphology of Sperm—Sperm was displayed over a slide, dried at room temperature, and then fixed in 75% ethanol for Harris-Schorr staining. Motility of sperm was assessed with computer-assisted motility analysis. Non-capacitated sperm suspension was immediately placed onto an analysis chamber (100 μm depth, Leja Products B.V., Netherlands) and kept at 37 °C for microscopic quantitative study of sperm movement. Sperm motility parameters were measured at 37 °C using a sperm analyzer (Hamilton Thorn Research, Beverly, MA). The settings employed for analysis were as follows: acquisition rate, 60 Hz; number of frames, 100; minimum contrast, 25; minimum cell size, 10; low static size gate, 2.4; high static size gate, 2.4; low static intensity gate, 1.02; high static intensity gate, 1.37; minimum elongation gate, 12; maximum elongation gate, 100; magnification factor, 0.70. The motility parameters measured were curvilinear velocity (VCL), average path velocity (VAP), and straight-line velocity (VSL). At least 100 motile sperm were analyzed for each assay. Motile sperm and progressive sperm were characterized by VAP >1 μm/s, by average path velocity >30 μm/s and straightness (VSL/VAP) >70%, respectively.

In Vitro Fertilization—Eggs were collected from mature OF1 females, synchronized with 5 units of pregnant mare serum gonadotrophin and 5 units of human chorionic gonadotrophin. Sperm were capacitated for 35–55 min in M16 2% BSA (37 °C, 5% CO_2) and introduced into droplets containing oocytes. Oocytes were incubated with 1.5×10^5 to 5×10^5 capacitated sperm/ml (37 °C, 5% CO_2) in M16 medium, and unbound sperm were washed away after 4 h of incubation. Twenty four hours after fertilization, the different stages, *i.e.* unfertilized oocytes, aborted embryos (corresponding to fragmented oocytes or oocytes blocked after the extrusion of the second polar body), and 2-cell embryos (as an indication of successful fertilization) were scored.

Capacitation and AR Triggering—Mouse sperm, obtained by manual trituration of caudae epididymides, were allowed to swim in M2 medium for 10 min and capacitated in M16 medium with 2% fatty acid-free BSA at 37 °C, 5% CO_2 for 65 min. For progesterone (P4) treatment, capacitated sperm (35 min) were incubated with P4 in M16 medium at 37 °C for the

last 30 min of capacitation (total duration of the experiment 65 min). Control experiments were always performed with the same concentration of DMSO in the medium (DMSO concentrations ranging from 0.01 to 0.1%).

AR Assay—Sperm were transferred in PBS solution and then fixed with 4% paraformaldehyde solution for 5 min. Sperm were washed (100 mM ammonium acetate, 2 min), wet mounted on slides, and air-dried. Slides were then rinsed with water and stained with Coomassie Blue (0.22%) for 2 min. Slides were analyzed, and at least 150 sperm were scored per condition.

Preparation of the Cumulus-Oocyte Complex-conditioned Medium for Enzyme Immunoassay—Eggs were collected from mature OF1 females (6 weeks old) synchronized with 5 units of pregnant mare serum gonadotrophin and 5 units of human chorionic gonadotrophin. Superovulation was confirmed by plasma P4 concentrations determined to be around 150 nM (154.4 ± 35.12 nM, $n = 5$). Cumulus-oocyte complexes harvested from 10 mice were placed in culture Petri dishes containing 250 μl of M16 medium and incubated for 10 min, 1 and 2 h at 37 °C in a 5% CO_2 atmosphere. Incubations were stopped by putting the dishes on ice and by centrifugation at 5,000 × g for 10 min at 4 °C. The supernatants and the cell pellets were frozen and used to determine the concentration of progesterone.

Determination of Progesterone Concentrations—Progesterone concentrations were determined by radioimmunoassay using ^{125}I-labeled progesterone (IBL International, Hamburg, Germany). The RIA detection limit was calculated to range between 0.1 and 0.5 ng/ml, *i.e.* between 0.3 and 1.6 nM depending upon the labeling lot. Cross-reactivity with other steroid hormones was reported to be minimal as follows: <3.5% for 20β-dihydroprogesterone and 5α-pregnane-3,20-dione; 1.5% for 17α-hydroxyprogesterone; 0.8% for 11-deoxycorticosterone; <0.4% for pregnenolone and corticosterone; and ≤0.1% for all other steroid hormones tested by the manufacturer. Of the steroids indicated, only 17α-hydroxyprogesterone is generated in significant amounts by cumulus cells. Its concentration is ~5-fold lower that of P4 in plasma during the luteal phase, and a 1.5% cross-reactivity with P4 can therefore not significantly bias the data. Briefly, after centrifugation the cell pellets were extracted with diethyl ether and centrifuged to remove cell debris. The ether extracts were evaporated under nitrogen, and the residues were re-dissolved in 250 μl of Tris buffer (10 mM, pH 7.4) containing 0.1% BSA. Culture medium (250 μl) and plasma samples were assayed directly according to the manufacturer's instructions. Progesterone levels were undetectable in the Tris/BSA buffer as well as in the M16 medium used for the incubations. For the calculation of intra-cumulus P4 concentrations, the total volume of the cumuli was estimated based on the number of oocytes per sample and on their average volume.

SDS-PAGE and Immunoblotting—Washed sperm were resuspended in Laemmli sample buffer without β-mercaptoethanol and boiled for 5 min. After centrifugation, 5% β-mercaptoethanol was added to the supernatants, and the mixture was boiled again for 5 min. Protein extracts equivalent to 1–2 × 10^6 sperm were loaded per lane and subjected to SDS-PAGE. Resolved proteins were transferred onto polyvinylidene difluoride membranes (Millipore). Membranes were treated with 20% fish skin gelatin (Sigma) in PBS-T and then incubated for 1 h at room temperature with anti-phosphotyrosine antibody (clone 4G10, Millipore, Molsheim, France) (1:10,000); this was followed by 1 h of incubation with a horseradish peroxidase-labeled secondary antibody. Immunoreactivity was detected using chemiluminescence detection kit reagents and a Chimidoc^{TM} Station (Bio-Rad, Marnes-la-Coquette, France).

Chemical Compounds—M2 medium, M16 medium, progesterone, and BSA were from Sigma (Lyon, France). Pregnant mare serum gonadotrophin and human chorionic gonadotrophin were from Intervet (Beaucouze, France), and BEL was from Interchim (Montluçon, France). Pyr-1 and LY329722 was provided by Prof. Michael Gelb (University of Washington, Seattle) and FKGK18 by George Kokotos (University of Athens, Greece).

Statistics —n represents the number of biological replicates, and for each replicate, more than 100 sperm were assessed per condition. Statistical analyses were performed with SigmaPlot. t tests were used to compare the effects of various compounds on AR and fertility. Data represent mean ± S.E. Statistical tests with 2-tailed p values of ≤0.05 were considered significant.

Results

Reproductive Phenotype of iPLA$_2\beta$, mGX, and cPLA$_2\alpha$ KO Males—We focused our study on iPLA$_2\beta$, mouse group X sPLA$_2$ (mGX), and cPLA$_2\alpha$ for the following reasons. First, iPLA$_2\beta$ and mGX have been shown to be present in mouse sperm (23, 24). Second, cPLA$_2\alpha$ is a constitutive enzyme with a ubiquitous expression and an important role in lipid mediator release and vesicle trafficking (38, 39), and more importantly its enzymatic activity and distribution are modified in patients presenting asthenozoospermia (26), suggesting that it may be important for male fertility. Deficient mice for these three proteins were previously described; the absence of the corresponding protein was confirmed, and their phenotype was studied (23, 36, 37). Nevertheless, the reproductive phenotype of *mGX* and *iPLA$_2\beta$* KO males was partially reported (23, 24), but no data are available for *cPLA$_2\alpha$* KO males. In Table 1, we present for the first time a comparative table showing several reproductive parameters of males from these three deficient mice. Both *iPLA$_2\beta$* and *mGX* KO males exhibit sperm defects with teratozoospermia and low motility (Table 1 and Fig. 1). iPLA$_2\beta$-deficient males were clearly the most affected, presenting deficient spermatogenesis as witnessed by the significant level of teratozoospermia (45% of typical sperm morphology *versus* 92% for WT sperm) and low motility, leading to complete *in vitro* infertility. The sperm phenotype of *mGX* KO males was less severe, with 70% of typical sperm morphology and half-reduction of progressive sperm, leading to a significant decrease of *in vitro* fertilization outcome (Table 1 and Fig. 1). In contrast, *cPLA$_2\alpha$* KO males presented a normal spermatocytogram and fertility, although mobility was affected. These latter results suggest that cPLA$_2\alpha$ is dispensable. However, its involvement in AR may be revealed only under specific conditions, as shown for *Pkdrej* KO mice for which the defective reproductive phenotype was revealed only under specific competing conditions (40). For this

TABLE 1

Phenotype of sperm from *mGX*, *iPLA$_2\beta$*, and *cPLA$_2\alpha$* KO males

Sperm count, sperm motility, sperm morphology, and ability to fertilize eggs *in vitro* were assessed. ND means not determined. Statistic analyses were conducted using *t* test.

	mGX KO $n = 3$	*iPLA$_2\beta$* KO $n = 3$	*cPLA$_2\alpha$* KO $n = 3$	Range values for WT sperm
Sperm cells concentration (millions/ml)	9.7	4.2[a]	9.8	**10–16**
Motility analysis				
Total motility (%)	14.0[a]	5.6[a]	30.0[a]	53–60
Progressive motility (%)	12.1[a]	2.0[a]	22.3[a]	43–48
Curvilinear velocity (VCL) mean (μm/s)	235.4	110.9[a]	183.0	175–260
Morphology analysis				
Typical morphology (%)	69[a]	45[a]	81	74–92
Head anomalies (%)	24[a]	44[a]	12	4–25
Midpiece anomalies (%)	5	7	1	ND
Flagellum anomalies (%)	10	18	6	ND
Absence of acrosome (%)	13.5	20.5[a]	14	13.5
Fertility analysis (*in vitro* fertilization)				
% of 2-cell embryos at 24 h KO male × WT female	17.2[a] ($n = 4$)	0.1[a] ($n = 6$)	52.5 ($n = 2$)	51 ($n = 10$)

[a] $p < 0.05$ as compared with WT sperm.

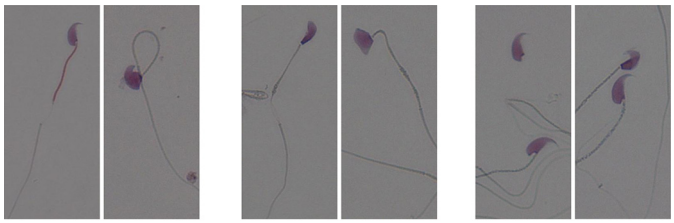

mGX KO *iPLA$_2\beta$* KO *cPLA$_2\alpha$* KO

FIGURE 1. **Typical defects observed with sperm from *iPLA$_2\beta$*, *mGX*, and *cPLA$_2\alpha$* KO males.** Sperm were stained by the Harris-Shorr method. The % of defective sperm is indicated in Table 1.

reason, the involvement of cPLA$_2\alpha$ was also explored in the rest of this study.

Physiological Concentration of P4 Measured in Cumulus Mass Induces AR of Mouse Sperm—In the literature, although numerous concentrations of P4 have been tested to induce AR, from sub-micromolar to tens of micromolars, P4 at 10–15 μM is usually used (20, 25, 41, 42). These concentrations may, however, not represent the physiological concentrations met by the sperm during their journey to oocytes embedded in the cumulus mass. To fit such physiological conditions, it was thus important to evaluate physiological P4 concentrations in both the cumulus mass and the tubal fluid. Cumuli of 10 superovulated females were harvested and incubated for 120 min in the fertilization medium, and [P4] was measured after centrifugation in both the cumuli and in the incubation medium by radioimmunoassay. We found similar P4 concentrations in the cumuli (0.71 ± 0.08 μM ($n = 5$)) and in the fertilization medium (1.13 ± 0.27 μM ($n = 5$)). Moreover, incubation of cumuli for various time points indicates that P4 synthesis is stable for at least 2 h (Fig. 2*A*). The value found for cumuli should be representative of the physiological value. This may not be the case for the fertilization medium because tubal fertilization is a dynamic process in which tubal fluid undergoes a continuous turnover. Indeed, P4 upon its synthesis is partly metabolized into 17OH-progesterone, a precursor of androstenedione, and partly released into the extracellular fluid by passive diffusion as it is a lipophilic hormone. Part of the progesterone that is released further diffuses and can be metabolized by adjacent cells, with the rest being cleared by the flux of tubal fluid and by the bloodstream. It is therefore difficult to reproduce *in vitro* these *in vivo* conditions. In our experimental conditions, the only clearance mechanism is metabolism of P4 by the cumulus cells, and therefore the measured concentration reflects the maximal attainable concentrations of P4 *in vivo*. One can therefore reasonably assume that the [P4] surrounding the cumuli does not exceed low micromolar levels. As an example, P4 concentrations in tubal fluid were reported to range from 2 to 10 nM in rabbit (43) and from 50 to 100 nM (44) in hamster depending upon the phase of the oestrous cycle. In super-ovulation, these concentrations can be assumed to be higher, due to the maturation of many more follicles. Thus, sperm meet a P4 concentration gradient during its journey to oocytes, from sub-micromolar concentrations in the tubal fluid to low micromolar concentrations in the cumulus mass. For this reason, two concentrations of P4 were tested as follows: 10 μM, a concentration that has been tested in various reports, and also 2 μM, a concentration closer to the physiological one. AR was assessed with the Coomassie Blue protocol (Fig. 2*B*) (45). We next performed a dose-response experiment of the AR of intact sperm at the end of the capacitation period as a function of P4 concentration ([P4]), testing P4 concentrations between 0.1 and 50 μM (Fig. 2*C*). The dose-response curve is bell-shaped, and 10 μM P4 elicited the highest response with 65.1 ± 1.9% ($n = 5$) acrosome-reacted sperm after 30 min of incubation, likely explaining why such concentrations are generally used in reports studying molecular pathways involved in the AR. Remarkably, physiological concentration of P4 at 2 μM was potent and triggered AR of ~55% of intact sperm.

Inhibition or Absence of iPLA$_2\beta$ Reduces the P4-induced AR—We first evaluated the involvement of iPLA$_2\beta$ by measuring the inhibitory effect of BEL and FKGK18 on the P4-induced AR. These compounds were tested on sperm capacitated for 35 min and further incubated for 30 min with 2 or 10 μM P4, and the AR rate was compared with the level obtained in the absence of the tested drug. The two compounds are potent inhibitors of the P4-induced AR with similar inhibitory effects; at 2 μM P4 the induced AR is inhibited by ~25% ($n = 3–6$) and at 10 μM by ~20–30% ($n = 3–6$) (Fig. 3, *A* and *B*). These results suggest that iPLA$_2\beta$ is involved in the P4-induced AR in the mouse. To confirm this result, the acrosome reactions of sperm from KO males deficient in iPLA$_2\beta$ were analyzed and compared with

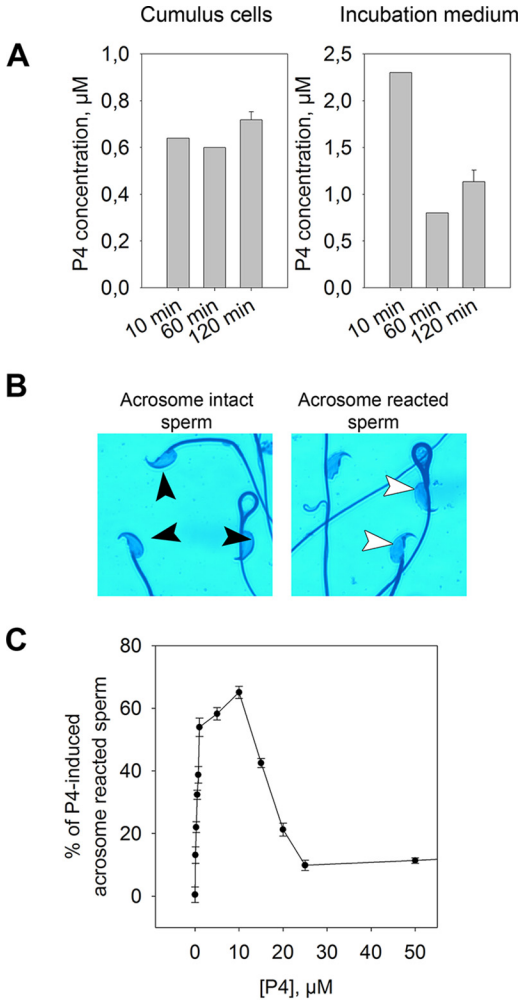

FIGURE 2. **Physiological concentration of P4 induces mouse AR.** *A,* determination of *ex vivo* [P4] in mouse cumulus mass. Harvested cumulus complexes were incubated for different times in M16 medium at 37 °C, 5% CO_2, and after centrifugation [P4] was measured in the cumulus or in the incubating medium at 10 ($n = 1$), 60 ($n = 1$), and 120 min ($n = 5$). *B,* sperm exocytosis was assessed by Coomassie Blue staining method, and non-acrosome-reacted sperm presented a dark blue crescent (*black arrowheads*), contrary to acrosome-reacted sperm (*white arrowheads*). *C,* dose-response curve of the AR to progesterone concentration ([P4]). Mouse sperm were capacitated for 35 min and treated with different [P4] for 30 min, and the % of P4-induced acrosome reacted sperm was determined by Coomassie Blue staining, $n = 5$. *n* represents the number of biological replicates and for each replicate, more than 100 sperm were assessed per condition.

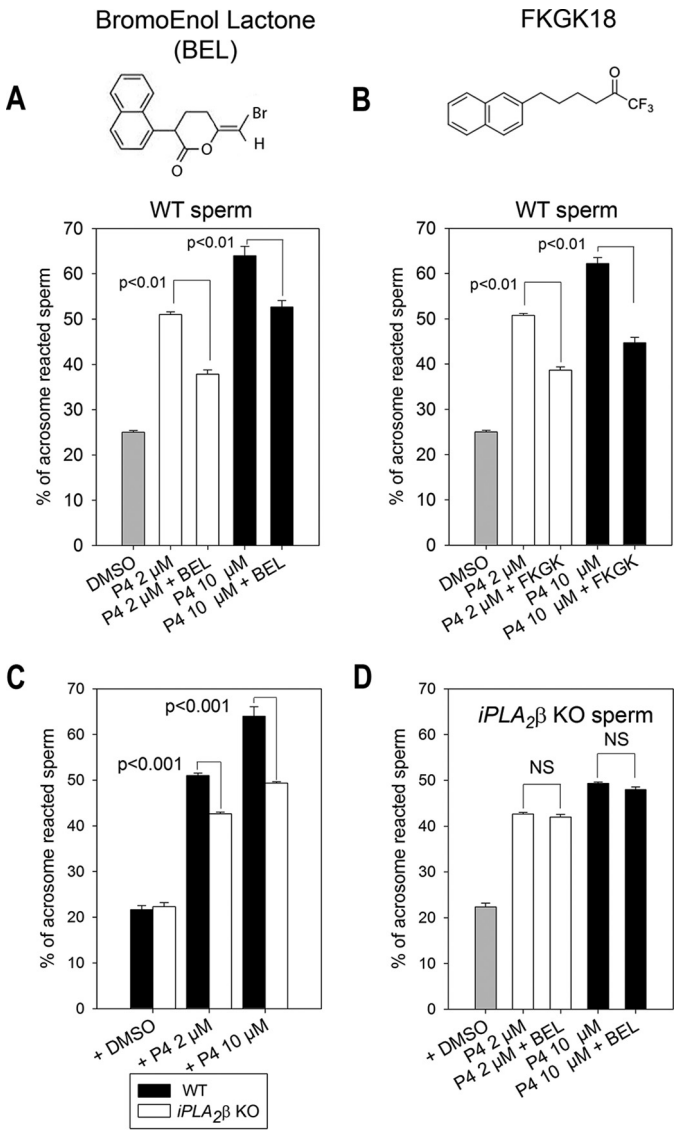

FIGURE 3. **iPLA$_2\beta$ inhibition, through pharmacological tools or genetically modified mice, leads to a decrease of P4-induced AR.** *A* and *B,* mouse sperm were capacitated for 35 min; the AR was triggered with 2 or 10 μM P4 for 30 min, and the % of acrosome reacted sperm was measured in the presence or absence of the iPLA$_2\beta$ inhibitors BEL at 10 μM (*A*) or FKGK18 at 10 μM, ($n = 3$) and whose chemical structure is presented on the top. DMSO corresponds to sperm capacitated for 35 min and further treated with DMSO only for 30 min. *C,* sperm from *iPLA$_2\beta$* KO mice were capacitated for 35 min, and the AR was triggered with P4 at 2 or 10 μM P4 for 30 min. The % of AR was then measured at the end of P4 treatment and compared with values obtained with WT littermate control mice ($n = 5$). *D,* potency of BEL on the AR of sperm from *iPLA$_2\beta$* KO mice. Sperm were capacitated for 35 min, and AR was triggered with P4 for 30 min at 2 or 10 μM P4. The % of AR was then measured at the end of P4 treatment in the presence or absence of 10 μM BEL ($n = 3$). *n* represents the number of biological replicates and for each replicate, more than 100 sperm were assessed per condition. Statistical differences were assessed using *t* test. *NS,* not significantly different.

those of control sperm from WT littermate males. Because these KO mice have a high level of teratozoospermia, we only took into account sperm exhibiting a normal head shape. The absence of the corresponding protein led to a decrease in the AR rate, and the percentage of decrease was close to those measured in pharmacological experiments (Fig. 3*C*), confirming the involvement of iPLA$_2\beta$ in P4-induced AR. Finally, the specificity of BEL was challenged by measuring its ability to inhibit the AR of sperm from *iPLA$_2\beta$* KO mice. BEL was no longer effective, demonstrating that its inhibitory effect on AR is mediated by iPLA$_2\beta$ (Fig. 3*D*). Altogether, these results demonstrate that iPLA$_2\beta$ contributes to P4-induced AR.

Inhibition or Absence of Mouse Group X sPLA$_2$ Reduces the P4-induced AR—Next, we evaluated the involvement of mGX sPLA$_2$ by measuring the inhibitory effect of LY329722 on the P4-induced AR as described above. LY32972, a pan inhibitor of sPLA$_2$, was a potent inhibitor of the P4-induced AR; at 2 μM the P4-induced AR is inhibited by ~30% ($n = 3$) and at 10 μM by ~35% ($n = 3$) (Fig. 4*A*). These results suggest that an sPLA$_2$ is involved in the P4-induced AR in the mouse. We assumed that it was most probably the sPLA$_2$ of group X (mGX), as we have previously shown that mGX is the only sPLA$_2$ in mouse sperm (24). To confirm this result, the acrosome reactions of sperm

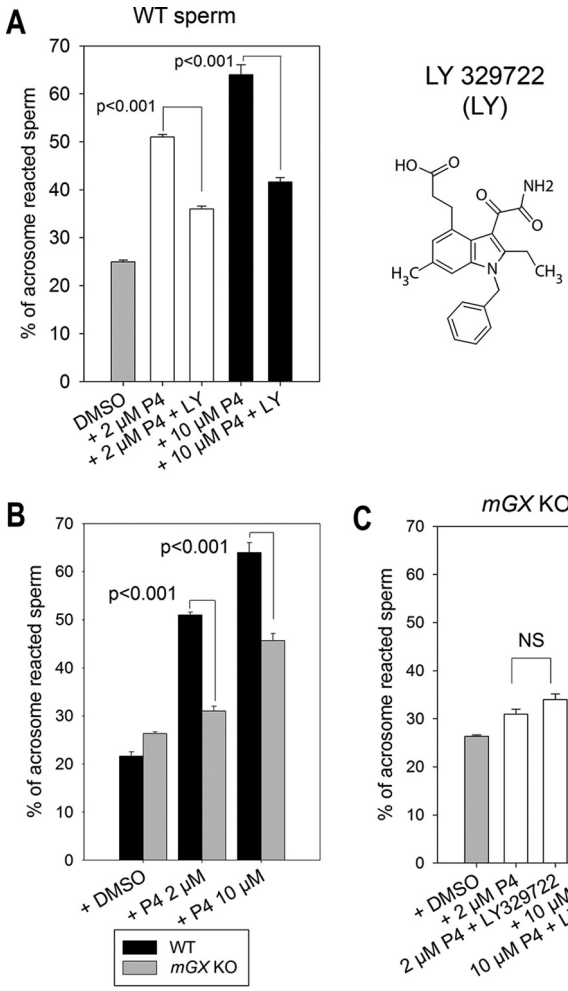

FIGURE 4. **Mouse group X sPLA$_2$ (mGX) inhibition, through pharmacological tools or genetically modified mice, leads to a decrease of P4-induced AR.** *A,* mouse sperm were capacitated for 35 min, and the AR was triggered with 2 or 10 μM P4 for 30 min, and the % of acrosome reacted sperm was measured in the presence or absence of the sPLA$_2$ inhibitor LY329722 (*LY*) at 1 μM (n = 3–6). DMSO corresponds to sperm capacitated for 35 min and further treated with DMSO only for 30 min. *B,* sperm from *mGX* KO mice were capacitated for 35 min, and the AR was triggered with P4 for 30 min at 2 or 10 μM P4. The % of AR was then measured at the end of P4 treatment and compared with values obtained with WT littermate control mice (n = 5). *C,* LY329722 does not inhibit the AR of sperm from *mGX* KO mice. Sperm were capacitated for 35 min, and AR was triggered with P4 for 30 min at 2 or 10 μM P4. The % of AR was then measured at the end of P4 treatment in the presence or absence of 1 μM LY329722 (n = 3). n represents the number of biological replicates, and for each replicate, more than 100 sperm were assessed per condition. Statistical differences were assessed using t test. *NS*, not significantly different.

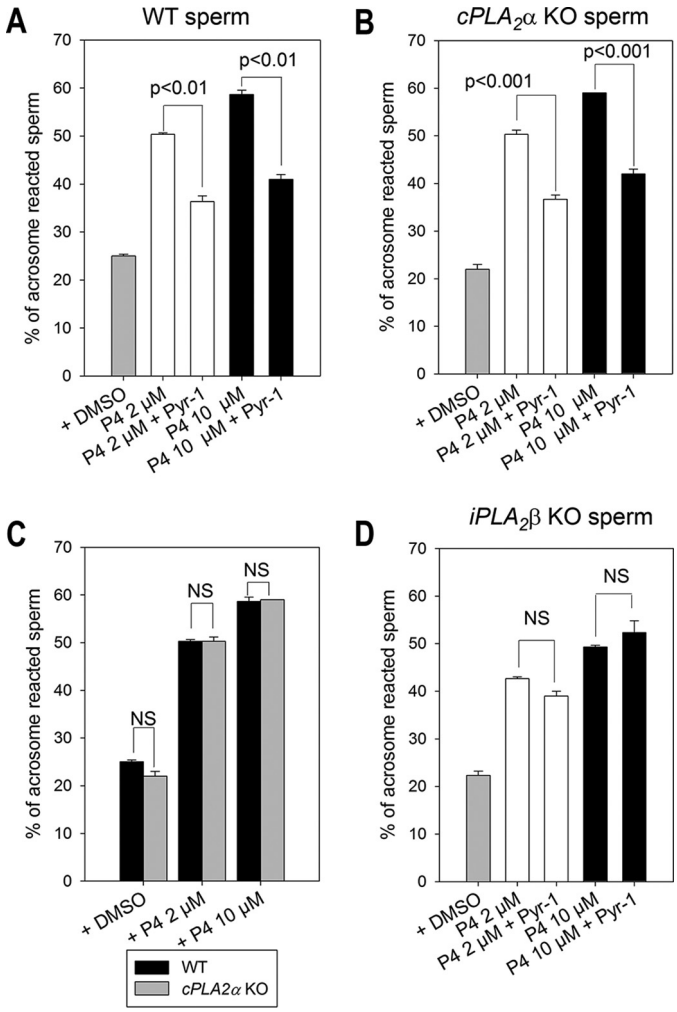

FIGURE 5. **cPLA$_2\alpha$ is not involved in P4-induced AR in mouse.** *A,* mouse sperm were capacitated for 35 min, and the AR was triggered with 2 or 10 μM P4 for 30 min, and the % of acrosome reacted sperm was measured in the presence or absence of the cPLA$_2\alpha$ inhibitor Pyr-1 at 1 μM (n = 3). DMSO corresponds to sperm capacitated for 35 min and further treated with DMSO only for 30 min. *B,* Pyr-1 is a potent inhibitor of the AR of sperm from *cPLA$_2\alpha$* KO mice. Sperm were capacitated for 35 min, and AR was triggered with P4 for 30 min at 2 or 10 μM P4. The % of AR was then measured at the end of P4 treatment in the presence or absence of 1 μM Pyr-1 (n = 3). *C,* sperm from *cPLA$_2\alpha$* KO mice were capacitated for 35 min, and the AR was triggered with P4 for 30 min at 2 or 10 μM P4. The % of AR was measured at the end of P4 treatment, and no difference was observed with values obtained with WT littermate control mice (n = 3). *D,* Pyr-1 does not inhibit the AR of sperm from *iPLA$_2\beta$* KO mice (n = 3) triggered by P4 for 30 min at 2 or 10 μM P4, suggesting that Pyr-1 actually inhibits iPLA$_2\beta$. n represents the number of biological replicates, and for each replicate more than 100 sperm were assessed per condition. Statistical differences were assessed using t test. *NS*, not significantly different.

from *mGX* KO males were analyzed and compared with those of control sperm from WT littermate males. The absence of mGX led to a decrease in the AR rate, and the percentage of decrease was close to that measured in pharmacological experiments (Fig. 4*B*), confirming the involvement of mGX in P4-induced AR. Finally, LY329722 was unable to inhibit the AR of *mGX* KO sperm, demonstrating that its inhibitory effect is mediated by mGX (Fig. 4*C*) and confirming that mGX is the only sPLA$_2$ involved in mouse AR. Altogether, these results demonstrate that mGX contributes to P4-induced AR.

cPLA$_2\alpha$ Is Not Involved in the P4-induced AR—We finally evaluated the involvement of cPLA$_2\alpha$ by measuring the inhibitory effect of Pyr-1 on the P4-induced AR as described for iPLA$_2\beta$. Pyr-1 was a potent inhibitor of the P4-induced AR; at 2 μM the P4 induced AR was inhibited by ~30% (n = 3) and at 10 μM by ~35% (n = 3) (Fig. 5*A*), suggesting that cPLA$_2\alpha$ is involved in the P4-induced AR in the mouse. However, Pyr-1 displayed the same inhibitory effect on both WT and *cPLA$_2\alpha$* KO sperm, suggesting that Pyr-1 is not specific for cPLA$_2\alpha$ (Fig. 5*B*). This latter result, associated with the fact that the AR rates of sperm from *cPLA$_2\alpha$* KO and WT males were similar (Fig. 5*C*), demonstrates that cPLA$_2\alpha$ is not involved in the mouse sperm AR and that at 1 μM, Pyr-1 inhibits the AR through an enzyme other than cPLA$_2\alpha$. Because this enzyme may be

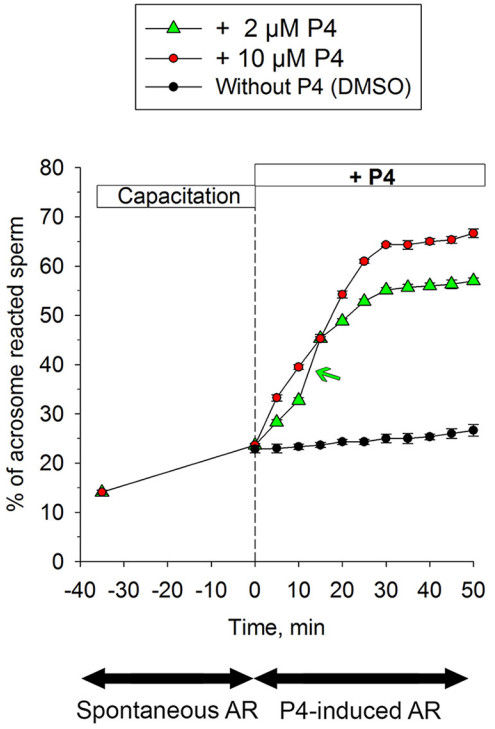

FIGURE 6. **Kinetic studies of AR of WT sperm.** Kinetic studies highlight a first phase of AR corresponding to SAR, occurring during the capacitation, and a second phase, corresponding to P4-induced AR. Sperm were capacitated during 35 min (−35 to 0 min), and P4 at 2 µM (*green triangles*, $n = 12$) or 10 µM (*red circles*, $n = 12$) was added into the capacitating medium (time 0, *dashed line*), and the % of completed AR was followed over 50 min. *Black circles* correspond to the % of acrosome-reacted sperm in medium containing DMSO (0.01–0.1%) only, without P4 ($n = 6$). The *green arrow* indicates the speeding up of slope observed between 10 and 15 min of AR induced by 2 µM P4.

iPLA$_2\beta$, the inhibitory effect of Pyr-1 was measured on sperm from *iPLA$_2\beta$ KO* mice; Pyr-1 was ineffective at blocking the AR (Fig. 5*D*), strongly suggesting that the target of Pyr-1 was actually iPLA$_2\beta$.

We have shown herein that iPLA$_2\beta$ and mGX inhibition, either through pharmacological tools or genetically modified mice, led to a decrease of the total P4-induced AR rate, demonstrating that these enzymes contribute to AR. In contrast, cPLA$_2\alpha$ does not participate with P4-induced AR in mouse.

Kinetic of AR Shows Different Types of AR and Different Sperm Subpopulations—Because the AR spreads over a long time period, the measure of the final AR rate 30 min after addition of P4 only gives a partial understanding of the mechanisms involved. To obtain better insight, the level of AR was plotted as a function of time from the beginning of the capacitation (time −35 min) to the end of the P4-induced AR period (up to 50 min), with time 0 corresponding to the addition of P4 into the capacitation medium (Fig. 6). After P4 addition, the AR rate was monitored every 5 min. This graph highlights two points. First, the level of AR of mouse epididymal sperm after collection was 14.08 ± 0.45 ($n = 24$). This ~15% likely corresponds to either poorly matured sperm or sperm stored in the epididymis for too long. Second, the kinetics revealed the presence of two types of AR, the spontaneous AR (SAR), which occurs during the capacitation period, and the P4-induced AR. Importantly, the AR kinetics highlight different sperm subpopulation; some sperm cells accomplish their AR very early after addition of P4 (<5 min), whereas others require longer incubation time with P4 (20–30 min). At 2 µM P4 (Fig. 6, *green triangles*, $n = 12$), analysis of the kinetics of the P4-induced AR suggests the involvement of different actors for the different subpopulations, because a significant speeding up of slope in the curve is observed between 10 and 15 min after P4 introduction to the medium compared with slope measured between 0 and 10 min (Fig. 6, highlighted by a *green arrow*). Moreover, the plateaux observed at 2 or 10 µM P4 show that a subpopulation of sperm (~45 and 30%, respectively) was insensitive to this agonist. Interestingly, at 10 µM P4 the kinetic of the AR is different (Fig. 6, *red circles*, $n = 12$); the initial AR increase (0–5 min) is stronger (as indicated by the comparison of slopes measured at 2 µM P4 *versus* that measured at 10 µM P4). Moreover, no change in the slope was observed between 0 and 30 min, suggesting that AR signaling may be different.

Spontaneous AR Is iPLA$_2\beta$-dependent—SAR, which is not well characterized yet, occurs in media supporting or not capacitation in the mouse and corresponds to sperm undergoing AR in the absence of any external stimulus. Although increased SAR was associated with bigger litter size in *CD46* KO mice (46), its physiological role remains elusive, because its rate greatly varies among species. We previously showed that during the first 45 min of capacitation, SAR is independent of mGX (24, 27). Nevertheless, another PLA$_2$ could be involved during the earlier phase of the SAR. To test this hypothesis, sperm were incubated between −35 and 0 min with the following PLA$_2$ inhibitors, BEL and FKGK18 for iPLA$_2\beta$ and LY329722 for mGX. Among the three different inhibitors, only those targeting iPLA$_2\beta$ were able to inhibit the SAR (Fig. 7*A*), showing that iPLA$_2\beta$ is activated during capacitation and is necessary to trigger the SAR. We also measured the rate of SAR in similar conditions (35 min of capacitation) of sperm from *iPLA$_2\beta$*, *mGX* and *cPLA$_2\alpha$* KO mice (Fig. 7*B*). For *mGX* and *cPLA$_2\alpha$* KO sperm, the absence of these proteins did not prevent the occurrence of SAR, confirming that these enzymes are not involved in SAR. For iPLA$_2\beta$, the level of AR at $t = -35$ min was already high in KO mice (20.6 ± 0.6%, $n = 4$) compared with WT littermates (14.3 ± 0.8%, $n = 4$), due to defective spermatogenesis (Fig. 1). Thus, experiments with *iPLA$_2\beta$* KO mice were not informative to determine the role of this protein in SAR. Finally, the inhibition of SAR observed with sperm incubated with BEL is unlikely to be due to an absence of capacitation because protein phosphorylation on tyrosine residues was observed with BEL, albeit slightly weaker (Fig. 7*C*).

Kinetic of AR Highlights That iPLA$_2\beta$ Is Necessary for the Initial Phase of the AR at Low P4 Concentration—We next assessed when and for how long iPLA$_2\beta$ is required during AR induced by 2 µM P4. Time window of its involvement was determined by measuring the kinetics of AR in the presence of the iPLA$_2\beta$ inhibitors BEL or FKGK18. As expected, during the capacitation (−35 to 0 min), the SAR is blocked, and in these conditions, the rate of AR at $t = 0$ is lower than that of sperm incubated in control conditions (Fig. 8*A*). For P4-induced AR, we focused our attention on two phases, corresponding to the fast responding subpopulation (0–5 min) and to the late responding subpopulation (20–30 min). The slopes of the two phases were measured allowing us to characterize the rise of AR

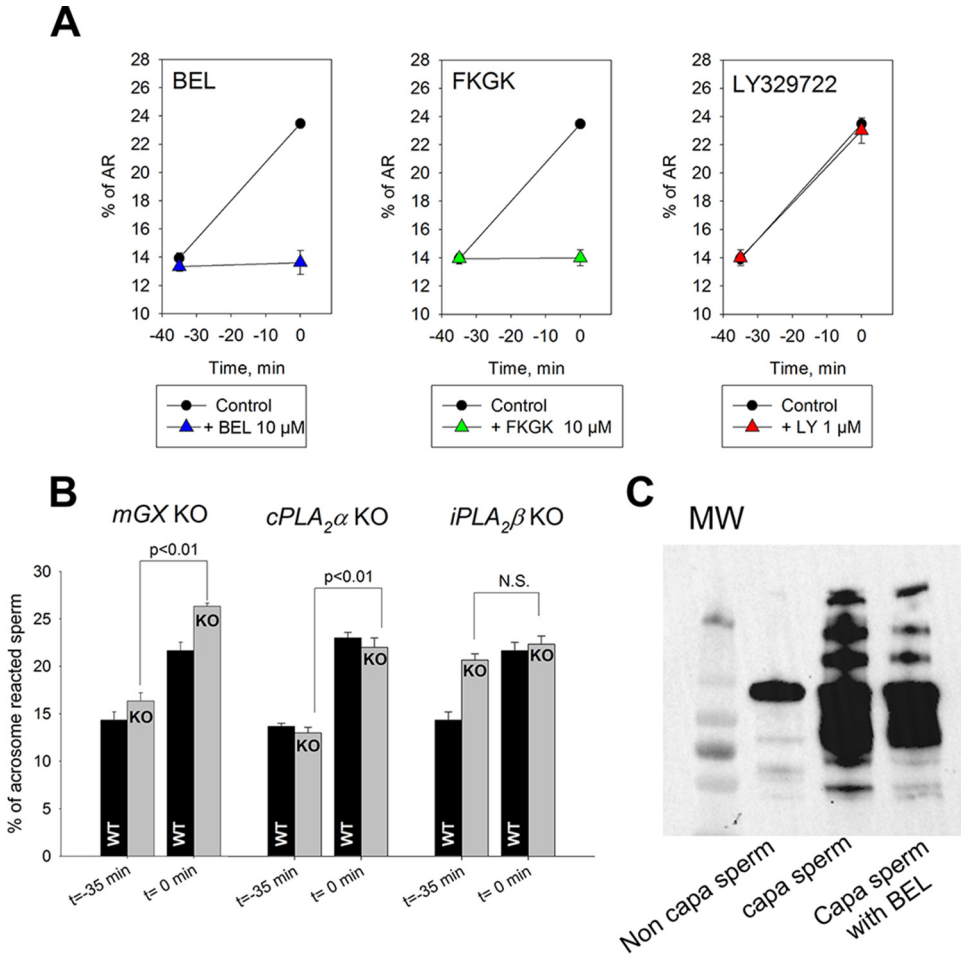

FIGURE 7. **iPLA$_2\beta$ is required for spontaneous AR.** *A,* iPLA$_2\beta$ inhibition blocks the spontaneous AR occurring during capacitation; BEL and FKGK18 but not LY329722 (*LY*) inhibited the spontaneous AR. The % of acrosome-reacted sperm was measured before capacitation (−35 min, *non capa*) or at the end of the capacitation period (0 min, *capa*) without PLA$_2$ inhibitors (*black circles*) or in the presence of BEL (10 μM, $n = 5$), FKGK18 (10 μM, $n = 3$), or LY329722 (1 μM, $n = 5$). *B,* histogram showing the % of AR before the capacitation ($t = -35$ min), and at the end of the capacitation ($t = 0$) for *mGX*, *cPLA$_2\alpha$*, and *iPLA$_2\beta$* KO mice and their corresponding WT. *C,* effect of BEL on the appearance of the hallmark of capacitation, protein tyrosine phosphorylations. BEL treatment did not prevent tyrosine phosphorylation. *n* represents the number of biological replicates, and for each replicate, more than 100 sperm were assessed per condition. Statistical differences were assessed using *t* test. *N.S.*, not significantly.

in both subpopulations (Fig. 8*B*). The early phase was clearly inhibited by iPLA$_2\beta$ inhibitors, as shown by the significant differences of the slopes between control and treated sperm, whereas the late phase was unchanged by BEL and FKGK18 (Fig. 8*B*). Because iPLA$_2\beta$ inhibitors also inhibited the SAR (Fig. 7*A*), we wondered whether the inhibition of AR rise observed with BEL or FKGK18 at 0–5 min might be related to the SAR inhibition induced by the inhibitor treatment. To address this question, a new experimental design was tested, with BEL introduced at the end of the capacitation period (Fig. 8*C*). Remarkably, whenever the iPLA$_2\beta$ inhibitor BEL was introduced, the response to 2 μM P4 was clearly delayed, and no increase was observed during the first 5 min (Fig. 8*D*), demonstrating that BEL inhibition is independent on the level of SAR. It is worth noting that the speeding up of the slope observed with sperm in control conditions between 10 and 15 min (Fig. 6, *green arrow*) was abolished with BEL and FKGK18, and slopes measured at 10–15 min dropped from 2.51 ± 0.19 ($n = 12$) in control condition to 1.4 ± 0.11 and 1.33 ± 0.13 for BEL and FKGK18, respectively ($n = 3$); the difference between slopes being statistically different ($p = 0.015$ and 0.013, respectively). This result suggests that iPLA$_2\beta$ contributes to the AR during the first ~15 min after P4 addition. Altogether, the observed final inhibition of ~30% AR with BEL is thus due to the delayed response and the absence of slope increase between 10 and 15 min. Altogether, these experiments show that iPLA$_2\beta$ is necessary for the early phase (0–5 min), contributes to the second phase (5–15 min), and is dispensable to the late phase (20–30 min) of AR induced at physiological P4 concentration.

At 10 μM P4, contrary to what was observed for 2 μM P4, the inhibition of the early phase in the presence of iPLA$_2\beta$ inhibitors was not observed (Fig. 9*A*), and the slopes of AR measured in control conditions or with BEL were not statistically different (Fig. 9*B*), suggesting that at this P4 concentration iPLA$_2\beta$ contributes slightly to the onset of the AR. In contrast to what was observed at low P4 concentration, the late phase (20–30 min) was significantly inhibited (Fig. 9*B*). Similar results were obtained with *iPLA$_2\beta$* KO mice (Fig. 10). At 2 μM P4, the slope of the initial rise (0–5 min) was significantly reduced in comparison with that obtained with WT sperm ($p < 0.001$), whereas the slope of the late phase of AR was unchanged (Fig 10, *A* and *B*). At 10 μM P4, no difference was

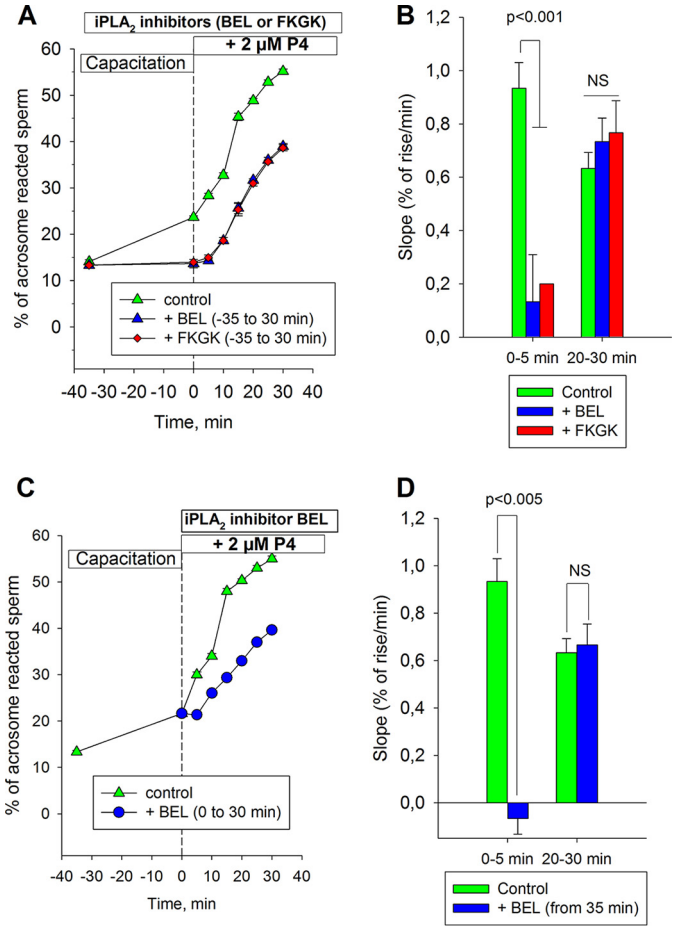

FIGURE 8. **Kinetic studies reveal that activation of iPLA$_2\beta$ is necessary for sperm achieving early AR at physiological P4 concentration.** *A,* after 35 min of capacitation, 2 μM P4 was introduced to the capacitating medium (time 0, *dashed line*), and the % of completed AR was followed during 30 min. BEL (10 μM, $n = 3$) or FKGK18 (10 μM, $n = 3$) was introduced at the beginning of the capacitation period. *Green triangles* correspond to the kinetic of the P4-induced AR of WT sperm measured in the absence of the inhibitors ($n = 12$). Notably, inhibition of the spontaneous AR by BEL or FKGK18 is clearly evidenced by the shift of the curve at $t = 0$. *B,* increase of AR was characterized by the measure of slopes of the curves between 0–5 and 20–30 min, corresponding to early and late response to P4, and calculated as $(x_5 - x_0)/(y_5 - y_0)$ and $(x_{30} - x_{20})/(y_{30} - y_{20})$, respectively. BEL and FKGK18 treatment inhibited the early increase, although no differences were observed between 20 and 30 min. *C,* similar experiment but BEL (10 μM) was introduced at the end (*blue circles,* $n = 3$) of the capacitation period. Because BEL was introduced at the end of the capacitation, no shift was observed at $t = 0$. *D,* AR increase was similarly characterized by measuring slopes between 0–5 and 20–30 min. Likewise, BEL treatment inhibited the early increase, although no difference was observed between 20 and 30 min. *n* represents the number of biological replicates, and for each replicate, more than 100 sperm were assessed per condition. Statistical differences were assessed using *t* test. *NS,* not significantly different.

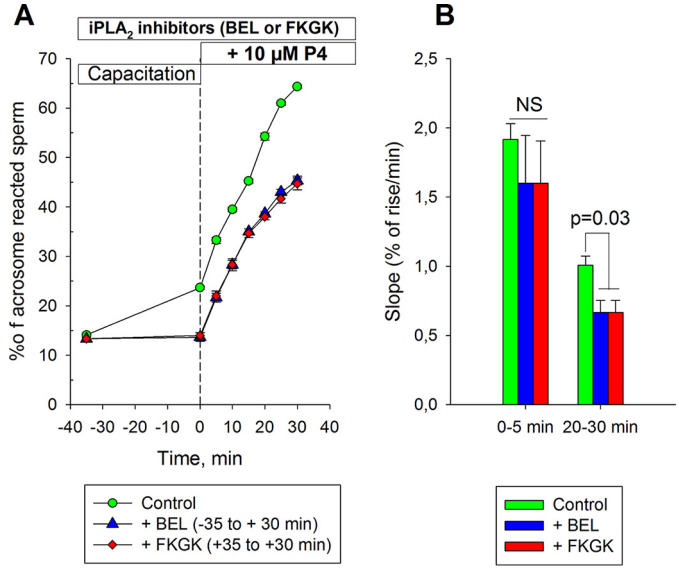

FIGURE 9. **Time window of the involvement of iPLA$_2\beta$ during AR is P4 concentration-dependent.** *A,* kinetic of AR induced by 10 μM P4. After 35 min of capacitation, P4 was introduced into the capacitating medium (time 0, *dashed line*), and the % of completed AR was followed during 30 min. BEL (10 μM, $n = 3$) or FKGK18 (10 μM, $n = 3$) was introduced at the beginning of the capacitation period. *Green circles* correspond to the kinetic of the P4-induced AR of WT sperm measured in the absence of iPLA$_2\beta$ inhibitors ($n = 12$). Notably, inhibition of the spontaneous AR by BEL or FKGK18 is clearly evidenced by the shift of the curve at $t = 0$. *B,* increase of AR was characterized by the measure of slopes of the curves between 0–5 and 20–30 min and corresponding to early and late response to P4 and calculated as $(x_5 - x_0)/(y_5 - y_0)$ and $(x_{30} - x_{20})/(y_{30} - y_{20})$, respectively. BEL or FKGK18 treatment inhibited the late increase of AR, and no differences were observed between 0 and 5 min. *n* represented the number of biological replicates, and for each replicate more than 100 sperm were assessed per condition. Statistical differences were assessed using *t* test. *NS,* not significantly different.

observed for 0–5 min, although a significant difference of the slope of AR increase was observed between WT and KO sperm during the late phase, confirming the results obtained with BEL and FKGK18. Importantly, results obtained with pharmacological tools or deficient animal show that the time window of the involvement of iPLA$_2\beta$ during AR is P4 concentration-dependent.

AR Inhibition by the sPLA$_2$ Inhibitor LY329722 Is P4 Concentration-dependent—We next assessed when and for how long mGX is required during P4-induced AR. The time course of activation was determined by measuring AR kinetics in the presence of LY329722 and by comparing the kinetics of AR of *mGX* KO and WT sperm. Contrary to what was observed when iPLA$_2\beta$ is inhibited, the AR of the fast responding sperm cells was not modulated by LY329722 or when mGX was genetically altered at low P4 concentration (Fig. 11*A*), and no statistical differences were found between slopes of P4-induced rise of AR in the different conditions tested between 0 and 5 min (Fig. 11*B*), confirming that mGX is dispensable to the early phase of AR. In contrast, the AR of late responding sperm cells (20–30 min) was blocked by LY329722 for WT sperm and inhibited for *mGX* KO sperm (Fig. 11, *A* and *B*). Moreover, from 10 min, the rise of AR was significantly reduced. These results thus show that mGX is necessary for the intermediate and late phase of AR, from 10 min.

Similar results were obtained at 10 μM P4; the early phase of AR (0–5 min) was not inhibited by LY329722 or changed with sperm from mGX-deficient mice, whereas the late phase was strongly inhibited in both conditions (Fig. 11, *C* and *D*).

Importantly, the overall inhibition measured at 30 min was more pronounced at 2 μM than 10 μM, with 68 and 56% of inhibition, respectively (Fig. 11, *A versus* B), suggesting that different pathways are activated at different P4 concentrations. To address this hypothesis, we measured AR inhibition by LY329722 as a function of P4 concentration. For P4 concentrations below 1 μM, LY329722 inhibition was very strong, and the AR was almost completely abolished (Fig. 12). In contrast, the potency of LY329722 decreased when P4 concentration

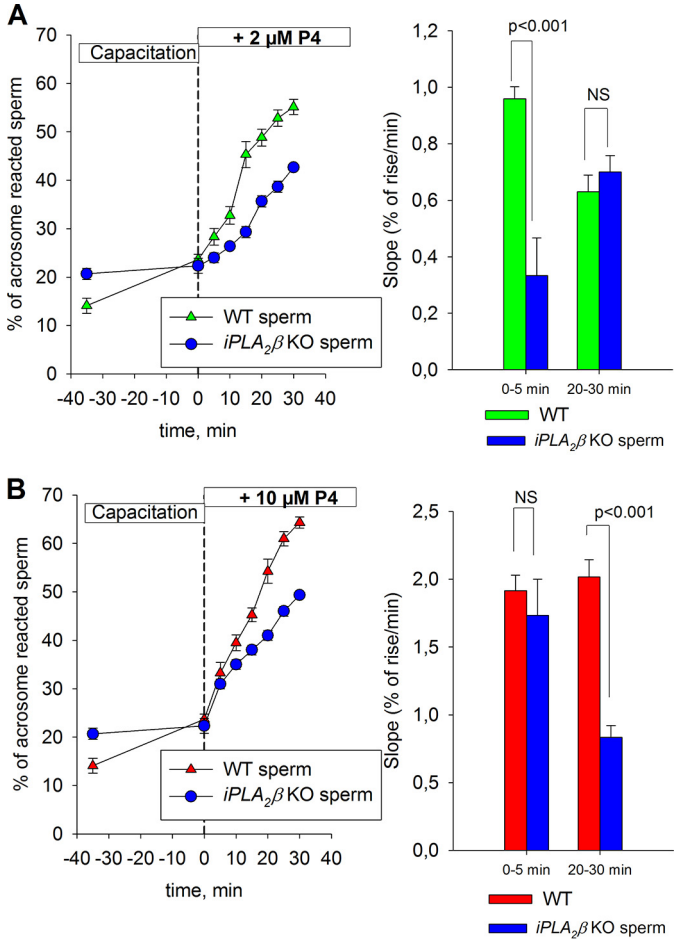

FIGURE 10. **Kinetics of the AR of sperm from *iPLA$_2$β* KO mice.** *A*, kinetic of AR induced by 2 μM P4. After 35 min of capacitation, P4 was introduced to the capacitating medium (time 0), and the % of AR of sperm from *iPLA$_2$β* KO mice was followed for 30 min (*blue circles*, $n = 3$). Kinetic of sperm from WT males is plotted on the same graph (*green triangles*, $n = 12$). *B*, increase of AR was objectified by the measure of slopes of the curves between 0–5 and 20–30 min, corresponding to early and late response to P4, and calculated as $(x_5 - x_0)/(y_5 - y_0)$ and $(x_{30} - x_{20})/(y_{30} - y_{20})$, respectively. *C* and *D*, similar experiments and analyses performed with 10 μM P4. *Red triangles* correspond to WT sperm ($n = 12$) and *blue circles* to sperm from *iPLA$_2$β* KO mice ($n = 3$). *n* represents the number of biological replicates, and for each replicate, more than 100 sperm were assessed per condition. Statistical differences were assessed using *t* test. *NS*, not significantly different.

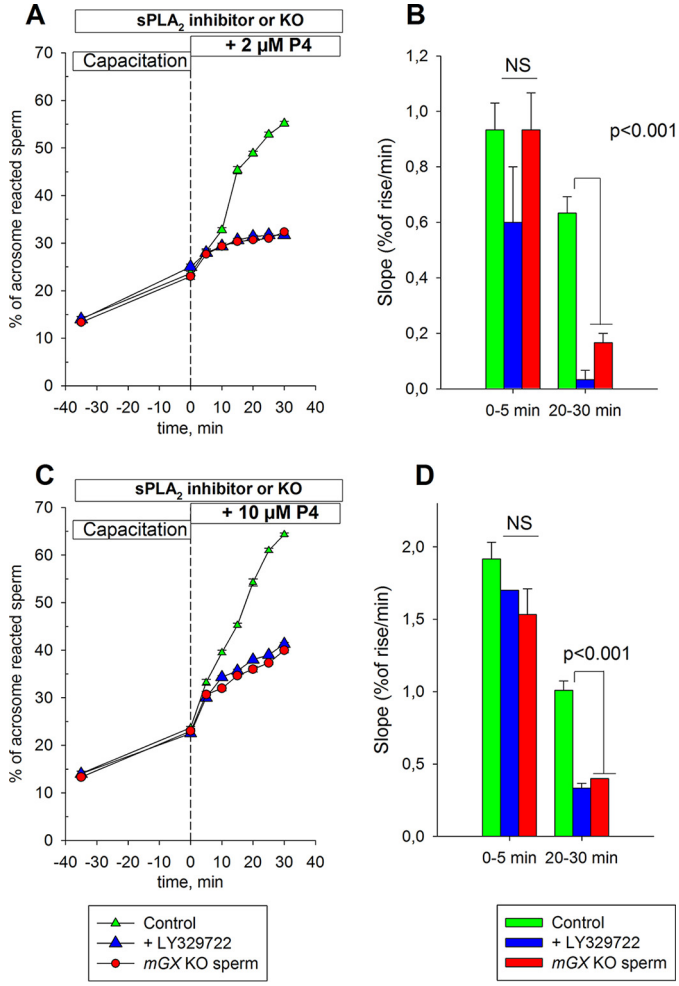

FIGURE 11. **Kinetic studies reveal that activation of mouse group X sPLA$_2$ is necessary for sperm cell achieving late AR induced by 2 or 10 μM P4.** *A*, after 35 min of capacitation, 2 μM P4 was introduced to the capacitating medium (time 0, *dashed line*), and the % of completed AR was followed over 30 min. LY329722 (1 μM) was introduced at the beginning of the capacitation period (*blue triangles*, $n = 3$). Sperm from mGX KO mice presented a similar AR kinetic (*red circles*, $n = 3$). *Green triangles* correspond to the kinetic of P4-induced AR of WT sperm measured in the absence of LY329722 ($n = 12$). *B*, increase of AR was characterized by the measure of slopes of the curves between 0–5 and 20–30 min, corresponding to early and late response to P4, and calculated as $(x_5 - x_0)/(y_5 - y_0)$ and $(x_{30} - x_{20})/(y_{30} - y_{20})$, respectively. mGX inhibition, either with a pharmacological tool or using sperm from deficient mice, inhibited the late increase of AR whereas no difference was observed between 0 and 5 min. *C* and *D*, similar experiments and analyses performed with 10 μM P4 ($n = 3$) and showing that mGX is necessary for the late phase of AR irrespectively to P4 concentration. *n* represents the number of biological replicates and for each replicate, more than 100 sperm were assessed per condition. Statistical differences were assessed using *t* test. *NS*, not significantly different.

increased above 1 μM, strongly suggesting that an alternative sPLA$_2$-independent AR pathway is activated at high concentrations of P4.

Inhibition of Both iPLA$_2$β and mGX Dramatically Reduces AR at Low P4 Concentration—We have clearly shown above that iPLA$_2$β and mGX are sequentially involved at low P4 concentration. iPLA$_2$β is necessary for the fast responding subpopulation (0–5 min) and contributes to sustain AR up to ~15 min. In contrast, mGX is dispensable for the early phase but is necessary for sperm accomplishing their AR after 10 min. To confirm these time windows of involvement, both iPLA$_2$β and mGX were inhibited at the same time, either by pharmacological tools or by a combination of inhibitor and KO mice; WT sperm samples were treated with both LY329722 and BEL inhibitors, and *mGX* KO sperm were treated with BEL and *iPLA$_2$β* KO sperm with LY329722. In the three conditions, both the early (0–5 min) and late phase (20–30 min) of AR are inhibited (Fig. 13*A*), and significant differences between slopes of P4-induced rise of AR measured in control conditions and those measured with inhibitors and/or KO sperm were found at both early and late phases (Fig 13*B*).

Discussion

iPLA$_2$β and mGX sPLA$_2$ but Not cPLA$_2$α Are Involved in the Mouse AR—The importance of phospholipase activity in the sperm AR was demonstrated several decades ago (1). However, the molecular identities of the implicated PLA$_2$s were not determined. Here, we have challenged the involvement of three

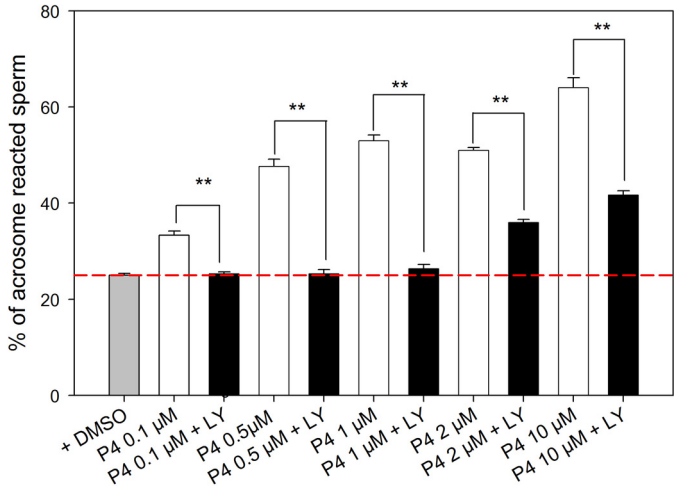

FIGURE 12. **Group X sPLA$_2$ is necessary for AR induced at P4 concentration below 1 μM.** The AR in the presence (*black columns*) or absence (*white columns*) of LY329722 (1 μM) was measured at 0.1, 0.5, 1, 2, and 10 μM P4 ($n = 3$), and their comparisons show that the potency of AR inhibition by LY329722 changes in function of progesterone concentration. ** indicates the differences between P4 and P4 + inhibitor ($p < 0.001$–0.0001) are significant. The *red dashed line* indicates the level of spontaneous AR. *n* represents the number of biological replicates, and for each replicate, more than 100 sperm were assessed per condition. Statistical differences were assessed using *t* test.

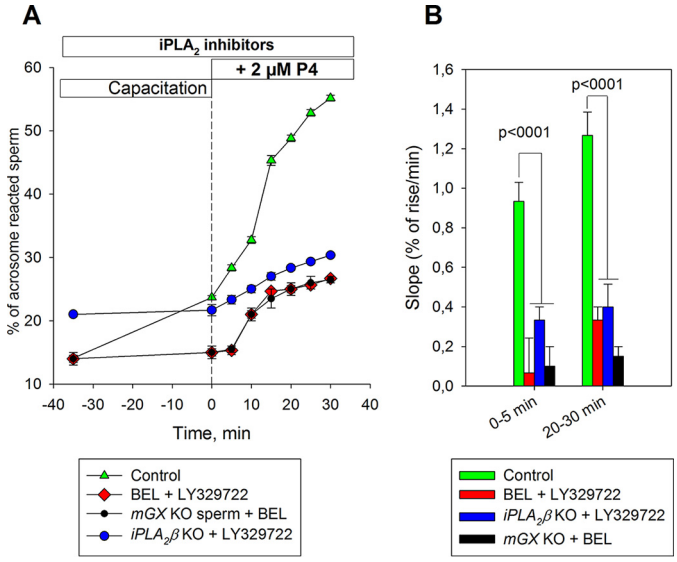

FIGURE 13. **Kinetic studies of the P4-induced AR reveal additive effect of iPLA$_2\beta$ and mGX sPLA$_2$ inhibition.** *A,* after 35 min of capacitation, 2 μM P4 was introduced to the capacitating medium (time 0, *dashed line*) and the % of completed AR was followed for 30 min. BEL (10 μM) and LY329722 (1 μM) were introduced at the beginning of the capacitation period. Three conditions were compared. (i) WT sperm were treated with BEL and LY329722 at the same time (*red diamond, n* = 3). (ii) sperm from *mGX* KO males were treated with BEL (*black circles, n* = 3). (iii) sperm from iPLA$_2\beta$ were treated with LY329722 (*blue circles, n* = 3). *Green triangles* correspond to the kinetic of the P4-induced AR of WT sperm measured under control conditions, without the PLA$_2$ inhibitors ($n = 12$). *B,* corresponding slopes at 0–5 and 20–30 min, showing additive effect of iPLA$_2\beta$ and mGX sPLA$_2$ inhibition. *n* represents the number of biological replicates, and for each replicate, more than 100 sperm were assessed per condition. Statistical differences were assessed using *t* test.

different PLA$_2$s as follows: iPLA$_2\beta$, cPLA$_2\alpha$, and group X sPLA$_2$ in the mouse AR by using specific inhibitors and the corresponding knock-out mice. Concerning the specificity of the used inhibitors, it is worth noting that the specificity of both iPLA$_2\beta$ and sPLA$_2$ inhibitors was validated by their lack of inhibition in the corresponding KO sperm. Moreover, LY329722 does not inhibit iPLA$_2\beta$, becauseLY329722 has no effect on SAR, contrary to BEL and FKGK18, two iPLA$_2\beta$ inhibitors. Similarly, BEL does not inhibit recombinant mGX sPLA$_2$ (data not shown). Collectively, these results validate our pharmacological study performed with these two compounds. Moreover, we showed that Pyr-1 was not specific at 1 μM and also inhibited iPLA$_2\beta$. Altogether, from pharmacological data and study of the AR of sperm from three different *PLA$_2$* knock-out mouse strains, we demonstrated that iPLA$_2\beta$ and group X sPLA$_2$ are involved in the P4-induced AR in mouse sperm. In contrast, AR measured on sperm from cPLA$_2\alpha$ mice show that this PLA$_2$ is involved neither in spontaneous nor induced AR. Although the presence of other PLA$_2$s cannot be ruled out, the probability of their contribution in the AR is very low. Concerning sPLA$_2$s, we have previously shown that only mGX is present in mouse mature sperm (24). Concerning the other members of the iPLA$_2$ (γ δ, ϵ, ζ, and η) and cPLA$_2$ (β, γ δ, ϵ, and ζ) groups, no expression was found in the testes (22), and it is thus unlikely that they are involved in the AR. Nevertheless, the presence of other phospholipases generating fusogenic lipids is not excluded. Indeed, PLA$_1$ is present in sperm (47), and PLB and PLD$_1$ are activated during the AR (48, 49), possibly explaining why some sperm were still able to perform the AR although iPLA$_2\beta$ and mGX were inhibited (Fig. 13).

Studying P4-induced AR Kinetics Provides New Insights on AR Actors, Different Subpopulations Are Activated by Different Mechanisms—Most of the studies performed on the molecular pathways involved in the AR focus either on the first minutes of the AR (50–52) or on the final rate obtained after 20–30 min (20, 48, 53). Only a few studies presented kinetic data, mainly on a single cell basis, thus focusing on fast responding cells (54–56). However, sperm population is very heterogeneous, and the presence of sperm subpopulations with different degrees of maturity after capacitation completion is well documented in human and mouse (57–61). At the population level, AR is a long lasting event occurring over 30 min (Fig. 6*A*), and only kinetic studies can address the question whether the AR is an homogeneous event. For this study, we chose to follow the full release of the acrosomal vesicle as evidenced by Coomassie Blue staining as an indication of AR outcome. We showed that this method can discriminate between different phases of the AR, revealing very sensitive subpopulations completing their AR in less than 5 min, and others requiring up to 30 min. Here, we show for the first time that these subpopulations do not rely on the same molecular pathways to achieve the AR. At 2 μM P4, a concentration close to the physiological concentration inside the cumulus, we showed that inhibition of iPLA$_2\beta$ by BEL blocked the fast responding subpopulation (Figs. 8 and 10*A*). For this fast responding subpopulation, mGX activity was not necessary because LY329722 alone had no effect and the initial rise of AR rate in *mGX* KO sperm was similar to that of WT sperm (Fig. 11*A*). Interestingly, between 10 and 15 min, the slope of the AR rise in the presence of BEL was lower than that measured in control condition (Fig. 8*A*), showing that iPLA$_2\beta$ inhibition partially blocked the AR during this interval and thus suggesting that early lipid hydrolysis by iPLA$_2\beta$ was responsible for the speeding up of AR increase observed between 10 and 15

min in control conditions (Fig. 6, *green arrow*). In contrast, mGX inhibition by LY329722 led to a strong blocking of the AR after 5 min (Fig. 10), demonstrating the key role of this enzyme in the intermediate and late phase.

We can thus propose that at this low physiological P4 concentration, sperm achieving their AR early rely only on iPLA$_2\beta$, whereas sperm achieving their AR late rely mainly on mGX sPLA$_2$, and in between these two phases, both PLA$_2$s are important.

Contribution of PLA$_2$ Is Dependent on P4 Concentration—Remarkably, the potencies of PLA$_2$ inhibitors on the AR were dependent on P4 concentration. At low P4 concentration, the initial phase (0–5 min) was strongly dependent on the iPLA$_2\beta$ activity (Fig. 8). At high P4 concentration, inhibition of iPLA$_2\beta$ (Fig. 9) or its absence (Fig. 10*B*) only slightly decreased the level of AR. Similarly, mGX inhibition produced a near-complete inhibition (>95%) of the P4-induced AR at [P4] <1 μM and a weaker inhibition at 10 μM P4 (~50%) (Fig. 12). The AR induced by low P4 concentrations is thus strongly PLA$_2$-dependent. Moreover, these results suggest that there are alternative pathways allowing a bypass of the lack of fusogenic lipids produced by iPLA$_2\beta$ or mGX at high P4 concentration. Ca^{2+} plays a central role in the AR, and Kobori *et al.* (62) showed that low or high P4 concentrations activate different Ca^{2+} responses; for [P4] <5 μM sperm exhibiting only transient calcium increase contrary to [P4] >10 μM, where both transient and long lasting calcium increases were observed. We can thus postulate that Ca^{2+} signaling triggered by low [P4] is able to initiate the AR in a primed sperm subpopulation only in conjunction with the production of fusogenic lipids by iPLA$_2\beta$. At high [P4], AR onset relies on a likely stronger Ca^{2+} signaling that can trigger the AR without fusogenic lipids or with a different set of fusogenic lipids, which could be produced by PLA$_1$ (47), PLB (48), or PLD$_1$ (49). Alternatively, P4 may bind to a different receptor at high concentrations (63) and activate a different pathway.

It is worth noting that at low P4 concentrations (< 1 μM), inhibition of mGX sPLA$_2$ by LY329722 led to an almost complete inhibition of the AR (Fig. 12). This result suggests that the expected synergy between P4-induced Ca^{2+} increase and fusogenic lipids produced by iPLA$_2\beta$ is not sufficient to trigger a full AR, but rather produce transitional states of acrosomal exocytosis, allowing only transient opening of pores. These pores can open and close before the final loss of the acrosome as suggested previously (64). During this transient period, sperm visually appear to be "acrosome-intact" sperm. The inhibition of mGX, located in the sperm acrosome (24), likely through these pores, may prevent synergistic effects of fusogenic lipids produced by both PLA$_2$s leading to their complete opening and thus pores return to a closed state, leading to a blocking of the AR.

Importantly, we showed that physiological P4 concentration is closer to 1 than 10 μM (Fig. 2*A*), and our results clearly indicate that under physiological conditions both iPLA$_2\beta$ and group X sPLA$_2$ are key players of the mouse sperm AR. Overall, our results indicate that different molecular pathways are activated by different P4 concentrations during the AR and thus that [P4] is a key factor, which should be taken into account in P4-induced AR studies.

Requirement of PLA$_2$ during Capacitation—We showed that the SAR occurring during the first 35 min of the capacitation period was inhibited only by iPLA$_2\beta$ inhibitors and not by a pan sPLA$_2$ inhibitor (Fig. 7*B*), demonstrating that iPLA$_2\beta$ is required during capacitation.

Remarkably, comparison of the final rate of the AR at 30 min between the sperm treated before (Fig. 8*A*) or at the end of the capacitation (Fig. 8*C*) shows no statistical difference (39.0 ± 0.57 *versus* 39.6 ± 0.33, $n = 3$; $p = 0.8$), although the level of AR at $t = 0$ is different, due to SAR inhibition when iPLA$_2\beta$ is inhibited during capacitation (Fig. 7*A*). This result indicates that inhibition of iPLA$_2\beta$ during capacitation increased the slope of P4-induced AR rise, mean slopes being 0.73 and 1.03 (measured between 5 and 30 min after P4), whereas BEL is introduced at the beginning or at the end of the capacitation, respectively. This result thus suggests that the subpopulation of sperm, which should have achieved their AR during capacitation, was primed and waiting for a cofactor to achieve the AR, which may be Ca^{2+} influx triggered by P4.

In conclusion, the progesterone-induced AR is a long lasting event, spreading over 30 min in the mouse, and by performing kinetic analyses, we revealed new insight concerning the AR and showed the presence of different sperm subpopulations that do not rely on the same molecular pathways to achieve their AR. At low physiological P4 concentration, sperm achieving their AR early (0–5 min post progesterone) rely only on iPLA$_2\beta$, whereas sperm achieving their AR late (20–30 min post progesterone) rely on group X sPLA$_2$. We thus showed that the AR is not a homogeneous molecular process and instead changes over time. Moreover, we showed that PLA$_2$ involvement depends upon P4 concentration, PLA$_2$s being key actors at low P4 concentrations close to the physiological concentration (<2 μM) and less central at higher P4 concentrations above 10 μM.

Author Contributions—C. A., S. H., and G. L. conceived and coordinated the study and wrote the paper. R. A. N., S. Y., J. P. H., J. E., and G. M. performed and analyzed AR studies. P. F. R. and T. K. designed primers and performed genotyping of KO mice. S. B. designed, performed, and analyzed the experiments shown in Fig. 1*A*. J. T. provided the iPLA$_2\beta$ KO mice. G. K. provided FKGK18. P. F. R. revised the article critically. All authors reviewed the results and approved the final version of the manuscript.

Acknowledgments—We thank Lexicon Genetics Inc. for providing mGX-deficient mice and Miriam Kolko and Charlotte Taul Braendstrup (University of Copenhagen, Denmark) for iPLA$_2\beta$-deficient mice. We thank Prof. Michael Gelb (University of Washington) for providing LY329722 and pyrolline-1. We thank Marie Cristou-Kent for English correction.

References

1. Roldan, E. R., and Shi, Q. X. (2007) Sperm phospholipases and acrosomal exocytosis. *Front. Biosci.* **12,** 89–104
2. Florman, H. M., Jungnickel, M. K., and Sutton, K. A. (2008) Regulating the acrosome reaction. *Int. J. Dev. Biol.* **52,** 503–510
3. Bleil, J. D., and Wassarman, P. M. (1983) Sperm-egg interactions in the mouse: sequence of events and induction of the acrosome reaction by a zona pellucida glycoprotein. *Dev. Biol.* **95,** 317–324

4. Thomas, P., and Meizel, S. (1989) Phosphatidylinositol 4,5-bisphosphate hydrolysis in human sperm stimulated with follicular fluid or progesterone is dependent upon Ca^{2+} influx. *Biochem. J.* **264,** 539–546
5. Roldan, E. R., Murase, T., and Shi, Q. X. (1994) Exocytosis in spermatozoa in response to progesterone and zona pellucida. *Science* **266,** 1578–1581
6. Jin, M., Fujiwara, E., Kakiuchi, Y., Okabe, M., Satouh, Y., Baba, S. A., Chiba, K., and Hirohashi, N. (2011) Most fertilizing mouse spermatozoa begin their acrosome reaction before contact with the zona pellucida during *in vitro* fertilization. *Proc. Natl. Acad. Sci. U.S.A.* **108,** 4892–4896
7. Inoue, N., Satouh, Y., Ikawa, M., Okabe, M., and Yanagimachi, R. (2011) Acrosome-reacted mouse spermatozoa recovered from the perivitelline space can fertilize other eggs. *Proc. Natl. Acad. Sci. U.S.A.* **108,** 20008–20011
8. Michaut, M., De Blas, G., Tomes, C. N., Yunes, R., Fukuda, M., and Mayorga, L. S. (2001) Synaptotagmin VI participates in the acrosome reaction of human spermatozoa. *Dev. Biol.* **235,** 521–529
9. Hutt, D. M., Baltz, J. M., and Ngsee, J. K. (2005) Synaptotagmin VI and VIII and syntaxin 2 are essential for the mouse sperm acrosome reaction. *J. Biol. Chem.* **280,** 20197–20203
10. Jungnickel, M. K., Sutton, K. A., Wang, Y., and Florman, H. M. (2007) Phosphoinositide-dependent pathways in mouse sperm are regulated by egg ZP3 and drive the acrosome reaction. *Dev. Biol.* **304,** 116–126
11. Cohen, R., Buttke, D. E., Asano, A., Mukai, C., Nelson, J. L., Ren, D., Miller, R. J., Cohen-Kutner, M., Atlas, D., and Travis, A. J. (2014) Lipid modulation of calcium flux through CaV2.3 regulates acrosome exocytosis and fertilization. *Dev. Cell.* **28,** 310–321
12. Darszon, A., Nishigaki, T., Beltran, C., and Treviño, C. L. (2011) Calcium channels in the development, maturation, and function of spermatozoa. *Physiol. Rev.* **91,** 1305–1355
13. Darszon, A., Sánchez-Cárdenas, C., Orta, G., Sánchez-Tusie, A. A., Beltrán, C., López-González, I., Granados-González, G., and Treviño, C. L. (2012) Are TRP channels involved in sperm development and function? *Cell Tissue Res.* **349,** 749–764
14. Thakkar, J. K., East, J., Seyler, D., and Franson, R. C. (1983) Surface-active phospholipase A2 in mouse spermatozoa. *Biochim. Biophys. Acta* **754,** 44–50
15. Meizel, S., and Turner, K. O. (1983) Stimulation of an exocytotic event, the hamster sperm acrosome reaction, by cis-unsaturated fatty acids. *FEBS Lett.* **161,** 315–318
16. Fleming, A. D., and Yanagimachi, R. (1984) Evidence suggesting the importance of fatty acids and the fatty acid moieties of sperm membrane phospholipids in the acrosome reaction of guinea pig spermatozoa. *J. Exp. Zool.* **229,** 485–489
17. Llanos, M. N., Morales, P., and Riffo, M. S. (1993) Studies of lysophospholipids related to the hamster sperm acrosome reaction *in vitro*. *J. Exp. Zool.* **267,** 209–216
18. Roldan, E. R., and Fragio, C. (1993) Phospholipase A2 activation and subsequent exocytosis in the Ca^{2+}/ionophore-induced acrosome reaction of ram spermatozoa. *J. Biol. Chem.* **268,** 13962–13970
19. Shi, Q. X., Chen, W. Y., Yuan, Y. Y., Mao, L. Z., Yu, S. Q., Chen, A. J., Ni, Y., and Roldan, E. R. (2005) Progesterone primes zona pellucida-induced activation of phospholipase A2 during acrosomal exocytosis in guinea pig spermatozoa. *J. Cell. Physiol.* **205,** 344–354
20. Pietrobon, E. O., Soria, M., Domínguez, L. A., Monclus Mde, L., and Fornés, M. W. (2005) Simultaneous activation of PLA2 and PLC are required to promote acrosomal reaction stimulated by progesterone via G-proteins. *Mol. Reprod. Dev.* **70,** 58–63
21. Murakami, M., Taketomi, Y., Miki, Y., Sato, H., Hirabayashi, T., and Yamamoto, K. (2011) Recent progress in phospholipase A(2) research: from cells to animals to humans. *Prog. Lipid Res.* **50,** 152–192
22. Dennis, E. A., Cao, J., Hsu, Y. H., Magrioti, V., and Kokotos, G. (2011) Phospholipase A2 enzymes: physical structure, biological function, disease implication, chemical inhibition, and therapeutic intervention. *Chem. Rev.* **111,** 6130–6185
23. Bao, S., Miller, D. J., Ma, Z., Wohltmann, M., Eng, G., Ramanadham, S., Moley, K., and Turk, J. (2004) Male mice that do not express group VIA phospholipase A2 produce spermatozoa with impaired motility and have greatly reduced fertility. *J. Biol. Chem.* **279,** 38194–38200
24. Escoffier, J., Jemel, I., Tanemoto, A., Taketomi, Y., Payre, C., Coatrieux, C., Sato, H., Yamamoto, K., Masuda, S., Pernet-Gallay, K., Pierre, V., Hara, S., Murakami, M., De Waard, M., Lambeau, G., and Arnoult, C. (2010) Group X phospholipase A2 is released during sperm acrosome reaction and controls fertility outcome in mice. *J. Clin. Invest.* **120,** 1415–1428
25. Li, K., Jin, J. Y., Chen, W. Y., Shi, Q. X., Ni, Y., and Roldan, E. R. (2012) Secretory phospholipase A2 group IID is involved in progesterone-induced acrosomal exocytosis of human spermatozoa. *J. Androl.* **33,** 975–983
26. Anfuso, C. D., Olivieri, M., Bellanca, S., Salmeri, M., Motta, C., Scalia, M., Satriano, C., La, V. S., Burrello, N., Caporarello, N., Lupo, G., and Calogero, A. E. (2015) Asthenozoospermia and membrane remodeling enzymes: a new role for phospholipase A. *Andrology* **3,** 1173–1182
27. Escoffier, J., Pierre, V. J., Jemel, I., Munch, L., Boudhraa, Z., Ray, P. F., De Waard, M., Lambeau, G., and Arnoult, C. (2011) Group X secreted phospholipase A2 specifically decreases sperm motility in mice. *J. Cell. Physiol.* **226,** 2601–2609
28. Abi Nahed, R., Escoffier, J., Revel, C., Jeammet, L., Payré, C., Ray, P. F., Hennebicq, S., Lambeau, G., and Arnoult, C. (2014) The effect of group X secreted phospholipase A2 on fertilization outcome is specific and not mimicked by other secreted phospholipases A2 or progesterone. *Biochimie* **99,** 88–95
29. Hui, D. Y. (2012) Phospholipase A(2) enzymes in metabolic and cardiovascular diseases. *Curr. Opin. Lipidol.* **23,** 235–240
30. Murakami, M., and Lambeau, G. (2013) Emerging roles of secreted phospholipase A(2) enzymes: an update. *Biochimie* **95,** 43–50
31. Schevitz, R. W., Bach, N. J., Carlson, D. G., Chirgadze, N. Y., Clawson, D. K., Dillard, R. D., Draheim, S. E., Hartley, L. W., Jones, N. D., and Mihelich, E. D. (1995) Structure-based design of the first potent and selective inhibitor of human non-pancreatic secretory phospholipase A2. *Nat. Struct. Biol.* **2,** 458–465
32. Ackermann, E. J., Conde-Frieboes, K., and Dennis, E. A. (1995) Inhibition of macrophage Ca^{2+}-independent phospholipase A2 by bromoenol lactone and trifluoromethyl ketones. *J. Biol. Chem.* **270,** 445–450
33. Ali, T., Kokotos, G., Magrioti, V., Bone, R. N., Mobley, J. A., Hancock, W., and Ramanadham, S. (2013) Characterization of FKGK18 as inhibitor of group VIA Ca^{2+}-independent phospholipase A2 (iPLA2β): candidate drug for preventing beta-cell apoptosis and diabetes. *PLoS One* **8,** e71748
34. Ghomashchi, F., Stewart, A., Hefner, Y., Ramanadham, S., Turk, J., Leslie, C. C., and Gelb, M. H. (2001) A pyrrolidine-based specific inhibitor of cytosolic phospholipase A(2)α blocks arachidonic acid release in a variety of mammalian cells. *Biochim. Biophys. Acta* **1513,** 160–166
35. Shirai, Y., Balsinde, J., and Dennis, E. A. (2005) Localization and functional interrelationships among cytosolic Group IV, secreted Group V, and Ca^{2+}-independent Group VI phospholipase A2s in P388D1 macrophages using GFP/RFP constructs. *Biochim. Biophys. Acta* **1735,** 119–129
36. Henderson, W. R., Jr., Chi, E. Y., Bollinger, J. G., Tien, Y. T., Ye, X., Castelli, L., Rubtsov, Y. P., Singer, A. G., Chiang, G. K., Nevalainen, T., Rudensky, A. Y., and Gelb, M. H. (2007) Importance of group X-secreted phospholipase A2 in allergen-induced airway inflammation and remodeling in a mouse asthma model. *J. Exp. Med.* **204,** 865–877
37. Bonventre, J. V., Huang, Z., Taheri, M. R., O'Leary, E., Li, E., Moskowitz, M. A., and Sapirstein, A. (1997) Reduced fertility and postischaemic brain injury in mice deficient in cytosolic phospholipase A2. *Nature* **390,** 622–625
38. Clark, J. D., Lin, L. L., Kriz, R. W., Ramesha, C. S., Sultzman, L. A., Lin, A. Y., Milona, N., and Knopf, J. L. (1991) A novel arachidonic acid-selective cytosolic PLA2 contains a Ca^{2+}-dependent translocation domain with homology to PKC and GAP. *Cell* **65,** 1043–1051
39. Ha, K. D., Clarke, B. A., and Brown, W. J. (2012) Regulation of the Golgi complex by phospholipid remodeling enzymes. *Biochim. Biophys. Acta* **1821,** 1078–1088
40. Sutton, K. A., Jungnickel, M. K., and Florman, H. M. (2008) A polycystin-1 controls postcopulatory reproductive selection in mice. *Proc. Natl. Acad. Sci. U.S.A.* **105,** 8661–8666
41. Patrat, C., Serres, C., and Jouannet, P. (2000) Induction of a sodium ion influx by progesterone in human spermatozoa. *Biol. Reprod.* **62,** 1380–1386

42. Reid, A. T., Lord, T., Stanger, S. J., Roman, S. D., McCluskey, A., Robinson, P. J., Aitken, R. J., and Nixon, B. (2012) Dynamin regulates specific membrane fusion events necessary for acrosomal exocytosis in mouse spermatozoa. *J. Biol. Chem.* **287,** 37659–37672
43. Richardson, L. L., and Oliphant, G. (1981) Steroid concentrations in rabbit oviducal fluid during oestrus and pseudopregnancy. *J. Reprod. Fertil.* **62,** 427–431
44. Libersky, E. A., and Boatman, D. E. (1995) Effects of progesterone on *in vitro* sperm capacitation and egg penetration in the golden hamster. *Biol. Reprod.* **53,** 483–487
45. Cardullo, R. A., and Florman, H. M. (1993) Strategies and methods for evaluating acrosome reaction. *Methods Enzymol.* **225,** 136–153
46. Inoue, N., Ikawa, M., Nakanishi, T., Matsumoto, M., Nomura, M., Seya, T., and Okabe, M. (2003) Disruption of mouse CD46 causes an accelerated spontaneous acrosome reaction in sperm. *Mol. Cell. Biol.* **23,** 2614–2622
47. Hiramatsu, T., Sonoda, H., Takanezawa, Y., Morikawa, R., Ishida, M., Kasahara, K., Sanai, Y., Taguchi, R., Aoki, J., and Arai, H. (2003) Biochemical and molecular characterization of two phosphatidic acid-selective phospholipase A1s, mPA-PLA1α and mPA-PLA1β. *J. Biol. Chem.* **278,** 49438–49447
48. Asano, A., Nelson-Harrington, J. L., and Travis, A. J. (2013) Phospholipase B is activated in response to sterol removal and stimulates acrosome exocytosis in murine sperm. *J. Biol. Chem.* **288,** 28104–28115
49. Lopez, C. I., Pelletán, L. E., Suhaiman, L., De Blas, G. A., Vitale, N., Mayorga, L. S., and Belmonte, S. A. (2012) Diacylglycerol stimulates acrosomal exocytosis by feeding into a PKC- and PLD1-dependent positive loop that continuously supplies phosphatidylinositol 4,5-bisphosphate. *Biochim. Biophys. Acta* **1821,** 1186–1199
50. Rockwell, P. L., and Storey, B. T. (2000) Kinetics of onset of mouse sperm acrosome reaction induced by solubilized zona pellucida: fluorimetric determination of loss of pH gradient between acrosomal lumen and medium monitored by dapoxyl (2-aminoethyl) sulfonamide and of intracellular Ca^{2+} changes monitored by fluo-3. *Mol. Reprod. Dev.* **55,** 335–349
51. O'Toole, C. M., Arnoult, C., Darszon, A., Steinhardt, R. A., and Florman, H. M. (2000) Ca^{2+} entry through store-operated channels in mouse sperm is initiated by egg ZP3 and drives the acrosome reaction. *Mol. Biol. Cell* **11,** 1571–1584
52. Son, J. H., and Meizel, S. (2003) Evidence suggesting that the mouse sperm acrosome reaction initiated by the zona pellucida involves an α7 nicotinic acetylcholine receptor. *Biol. Reprod.* **68,** 1348–1353
53. Fukami, K., Yoshida, M., Inoue, T., Kurokawa, M., Fissore, R. A., Yoshida, N., Mikoshiba, K., and Takenawa, T. (2003) Phospholipase Cδ4 is required for Ca^{2+} mobilization essential for acrosome reaction in sperm. *J. Cell Biol.* **161,** 79–88
54. Harper, C. V., Cummerson, J. A., White, M. R., Publicover, S. J., and Johnson, P. M. (2008) Dynamic resolution of acrosomal exocytosis in human sperm. *J. Cell Sci.* **121,** 2130–2135
55. Buffone, M. G., Rodriguez-Miranda, E., Storey, B. T., and Gerton, G. L. (2009) Acrosomal exocytosis of mouse sperm progresses in a consistent direction in response to zona pellucida. *J. Cell. Physiol.* **220,** 611–620
56. Sosa, C. M., Pavarotti, M. A., Zanetti, M. N., Zoppino, F. C., De Blas, G. A., and Mayorga, L. S. (2015) Kinetics of human sperm acrosomal exocytosis. *Mol. Hum. Reprod.* **21,** 244–254
57. Perreault, S. D., and Rogers, B. J. (1982) Capacitation pattern of human spermatozoa. *Fertil. Steril.* **38,** 258–260
58. Zalata, A., Hassan, A., Christophe, A., Comhaire, F., and Mostafa, T. (2010) Cholesterol and desmosterol in two sperm populations separated on Sil-Select gradient. *Int. J. Androl.* **33,** 528–535
59. Cohen-Dayag, A., Tur-Kaspa, I., Dor, J., Mashiach, S., and Eisenbach, M. (1995) Sperm capacitation in humans is transient and correlates with chemotactic responsiveness to follicular factors. *Proc. Natl. Acad. Sci. U.S.A.* **92,** 11039–11043
60. Escoffier, J., Navarrete, F., Haddad, D., Santi, C. M., Darszon, A., and Visconti, P. E. (2015) Flow cytometry analysis reveals that only a subpopulation of mouse sperm undergoes hyperpolarization during capacitation. *Biol. Reprod.* **92,** 121
61. Maree, L., and van der Horst, G. (2013) Quantification and identification of sperm subpopulations using computer-aided sperm analysis and species-specific cut-off values for swimming speed. *Biotech. Histochem.* **88,** 181–193
62. Kobori, H., Miyazaki, S., and Kuwabara, Y. (2000) Characterization of intracellular Ca^{2+} increase in response to progesterone and cyclic nucleotides in mouse spermatozoa. *Biol. Reprod.* **63,** 113–120
63. Correia, J. N., Conner, S. J., and Kirkman-Brown, J. C. (2007) Non-genomic steroid actions in human spermatozoa. "Persistent tickling from a laden environment". *Semin. Reprod. Med.* **25,** 208–219
64. Kim, K. S., Foster, J. A., Kvasnicka, K. W., and Gerton, G. L. (2011) Transitional states of acrosomal exocytosis and proteolytic processing of the acrosomal matrix in guinea pig sperm. *Mol. Reprod. Dev.* **78,** 930–941